

## A Model of the Oscillatory Metabolism of Activated Neutrophils

Lars F. Olsen,<sup>\*†</sup> Ursula Kummer,<sup>\*</sup> Andrei L. Kindzelskii,<sup>‡</sup> and Howard R. Petty<sup>‡</sup>

<sup>\*</sup>European Media Laboratory, Schloss-Wolfsbrunnenweg 33, D-69118 Heidelberg, Germany; <sup>†</sup>Department of Biochemistry and Molecular Biology, Syddansk Universitet, DK-5230 Odense M, Denmark; and <sup>‡</sup>Department of Biological Sciences, Wayne State University, Detroit, Michigan 48202 USA

**ABSTRACT** We present a two-compartment model to explain the oscillatory behavior observed experimentally in activated neutrophils. Our model is based mainly on the peroxidase-oxidase reaction catalyzed by myeloperoxidase with melatonin as a cofactor and NADPH oxidase, a major protein in the phagosome membrane of the leukocyte. The model predicts that after activation of a neutrophil, an increase in the activity of the hexose monophosphate shunt and the delivery of myeloperoxidase into the phagosome results in oscillations in oxygen and NAD(P)H concentration. The period of oscillation changes from >200 s to 10–30 s. The model is consistent with previously reported oscillations in cell metabolism and oxidant production. Key features and predictions of the model were confirmed experimentally. The requirement of the hexose monophosphate pathway for 10 s oscillations was verified using 6-aminonicotinamide and dexamethasone, which are inhibitors of glucose-6-phosphate dehydrogenase. The role of the NADPH oxidase in promoting oscillations was confirmed by dose-response studies of the effect of diphenylene iodonium, an inhibitor of the NADPH oxidase. Moreover, the model predicted an increase in the amplitude of NADPH oscillations in the presence of melatonin, which was confirmed experimentally. Successful computer modeling of complex chemical dynamics within cells and their chemical perturbation will enhance our ability to identify new antiinflammatory compounds.

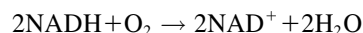
### INTRODUCTION

Neutrophilic leukocytes constitute our primary defense against invading pathogens. Upon bacterial invasion, neutrophils leave the bloodstream through transiently generated gaps between the endothelial cells and migrate actively toward the site of infection. Here they engulf and kill the bacteria. The process of phagocytosis continues until the bacterium is completely internalized, surrounded by membrane in the phagosome. The bacterium in the phagosome is destroyed by an arsenal of cytotoxic agents. Many of these digestive and antibacterial compounds originate from cytoplasmic granules that are emptied into the phagosome upon activation. Then follows a large burst in nonmitochondrial respiratory activity, much of which can be ascribed to the NADPH oxidase complex that assembles at the phagosomal membrane (Henderson and Chappell, 1996). Electrons are transferred from cytoplasmic NADPH to oxygen on the phagosomal side of the membrane, generating the so-called reactive oxygen species, e.g., superoxide, hydrogen peroxide, hydroxyl radical, and singlet oxygen. The NADPH used is itself produced by the hexose monophosphate shunt. Although there is good evidence that the respiratory burst is associated with NADPH oxidase activity, other proteins also participate in the oxidative destruction of targets. One protein is myeloperoxidase, which is, in fact, the most abundant protein of the neutrophil

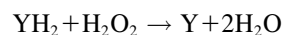
(Klebanoff, 1991). Myeloperoxidase, which is stored in the azurophilic granules from which it is released into the phagosome upon activation, is believed to catalyze the reaction of hydrogen peroxide with  $\text{Cl}^-$  ions to form HOCl, which also has antibacterial activity (Dunford, 1999; Hampton et al., 1998; Klebanoff, 1991).

Recently, it was shown that in migrating neutrophils the concentrations of NAD(P)H and reactive oxygen species oscillate (Petty, 2001; Amit et al., 1999). The mechanism responsible for such oscillations is not known. However, various known biochemical oscillators such as glycolysis and cytosolic calcium (Petty, 2001) have been proposed as sources of the oscillations. It is quite likely that several biochemical oscillators operate together to produce the experimentally observed oscillations. Here we wish to present evidence for another such oscillator that involves myeloperoxidase, melatonin, NADPH, and NADPH oxidase.

In a previous paper (Olsen et al., 2001) it was shown that melatonin activates the reaction:



catalyzed by horseradish peroxidase, lactoperoxidase, or soy bean peroxidase. This reaction is also known as the peroxidase-oxidase (PO) reaction (Scheeline et al., 1997). In addition to activating the PO reaction, melatonin also induces oscillations in this reaction when the pH is between 4 and 6. Because lactoperoxidase and myeloperoxidase are structurally very similar (Dunford, 1999) and because melatonin has been shown to be a substrate for the classical peroxidase reaction:



catalyzed by both horseradish peroxidase and myeloperoxidase (Silva et al., 2000; Allegra et al., 2001; Ximenes et al.,

*Submitted March 19, 2002, and accepted for publication September 4, 2002.*

Address reprint requests to Lars F. Olsen, Dept. of Biochemistry and Molecular Biology, Syddansk Universitet, Campusvej 55, DK-5230 Odense M, Denmark. Tel.: +45-6550-2482; Fax: +45-6550-2467; E-mail: lfo@dou.dk.

© 2003 by the Biophysical Society

0006-3495/03/01/69/13 \$2.00

2001), it is tempting to suggest that a myeloperoxidase-catalyzed PO reaction could also be involved in the oscillations in neutrophils. Myeloperoxidase has been shown to catalyze the PO reaction (Fujimoto et al., 1993). Furthermore, peroxidases do not discriminate between NADH and NADPH as the reducing substrate (Nakamura et al., 1969). Finally, it has been shown that leukocytes may synthesize melatonin (Finocchiaro et al., 1991).

Here we first study experimentally the PO reaction catalyzed by horseradish peroxidase enclosed in liposomes while the substrates NADH and  $O_2$  are continuously supplied to the external medium. Melatonin is added to the reaction mixture in order to mediate electron trafficking between NADH and peroxidase. We then use the experimental results to develop a model of the PO reaction catalyzed by myeloperoxidase in neutrophils. The computational results are tested by performing key experiments on neutrophils confirming the main results of the simulations.

## MATERIALS AND METHODS

### Materials

Reagents were obtained from Sigma-Aldrich (St. Louis, MO) unless otherwise noted. Horseradish peroxidase (330 units/mg, RZ = 3.0) and NADH (grade II) were purchased from Boehringer Mannheim, (Mannheim, Germany) whereas L- $\alpha$ -phosphatidylcholine (based on palmitoyl-oleoyl phosphatidylcholine) (>99%) was purchased from Avanti Polar Lipids (Alabaster, AL).

### Liposomes

Liposomes were made of palmitoyl-oleoyl phosphatidylcholine. The lipid was first dissolved in chloroform and placed in a vacuum chamber overnight. The resulting lipid film was then hydrated by adding an aqueous solution containing 20  $\mu$ M horseradish peroxidase and 0.1 M sodium acetate buffer, pH 5.1. The final concentration of lipid in the suspension was 10 mM. The lipid suspension was placed in a heating bath at 35°C for at least 2 h. The suspension was vigorously shaken from time to time. Unilamellar vesicles containing horseradish peroxidase were made by extrusion (MacDonald et al., 1991). The lipid suspension was passed through a Millipore HTTP (Millipore, Glostrup, Denmark) filter with a pore size of 0.4  $\mu$ M under an  $N_2$  pressure of 10 atmospheres 11 times. The liposomes were separated from the peroxidase-containing solution by elution through a Sephacryl S-200 HR (Amersham Biosciences, Hørsholm, Denmark) column using 0.1 M sodium acetate, pH 5.1, as the eluent.

### PO reaction

Experiments were conducted at 28 ( $\pm 0.1$ )°C in a 2.0  $\times$  2.0  $\times$  4.3 cm quartz cuvette fitted with a thermostating jacket. The cuvette was connected to a Zeiss Specord S 10 diode array spectrophotometer (Carl Zeiss, Jena, Germany) through optical fibers. Oxygen in the solution was measured with a Clark-type oxygen electrode (Microelectrodes, Bedford, NH). The reaction mixture consisted of an 8 ml well-stirred homogeneous aqueous solution containing 0.1 M sodium acetate, pH 5.1, 200  $\mu$ M melatonin and peroxidase-containing liposomes (see above).  $O_2$  is entering the reaction mixture from a 1.05% (v/v)  $O_2/N_2$  gas mixture above the liquid. The rate of diffusion into the liquid follows Fick's law and the oxygen transfer constant was measured as  $5.6 \times 10^{-3}$  ( $\pm 0.1 \times 10^{-3}$ ) s $^{-1}$  corresponding to a stirring rate of 900 ( $\pm 10$ ) rpm. NADH was supplied to the reaction mixture by infusion of a 0.1 M stock solution through a capillary whose tip was below

the surface of the liquid. The infusion was mediated by a Harvard Apparatus (Holliston, MA) model 22 infusion pump and the infusion rate was 35  $\mu$ l/h.

### Cells

Human peripheral blood neutrophils were prepared as previously described (Amit et al., 1999). Cells were suspended in Hanks' balanced salt solution containing glucose but not phenol red. Morphologically polarized cells with well-defined uropods, which are characteristics of cell motility, were examined.

### Detection of NAD(P)H oscillations

Metabolic oscillations were detected using NAD(P)H microscopy (Amit et al., 1999; Rosenspire et al. 2000). NAD(P)H autofluorescence was detected using narrow bandpass interference filters (AF series, Omega Optical, Brattleboro, VT) and a dichroic mirror. An iris diaphragm was adjusted to exclude light from neighboring cells. A cooled photomultiplier tube held in a Products for Research (Danvers, MA) housing attached to a Zeiss microscope was used (Rosenspire et al., 2000).

### Imaging spectrophotometry of chemiluminescence

Cells were observed microscopically at 37°C. Imaging spectrophotometry was performed using an Axiovert 135 fluorescence microscope with a quartz condenser and quartz objective (Carl Zeiss, New York). To increase light collection efficiency, the microscope's bottom port was employed. This port was fiberoptically coupled to the input of an Acton 150 (Acton Instruments, Acton, MA) imaging spectrophotometer (Petty et al., 2000). The exit side was connected to a liquid  $N_2$ -cooled intensifier attached to a Peltier-cooled IMAX-512 camera ( $-20^\circ$ C) (Princeton Instruments, Trenton, NJ). The camera was controlled by a high-speed Princeton ST-133 interface and a Stanford Research Systems (Sunnyvale, CA) DG-535 delay gate generator (Petty et al., 2000). A Dell Precision 410 workstation with an 800 MHz processor, 1.0 Gb RAM, 10 Mb onboard cache, and a high-speed Lava Dual PCI enhanced port (Rexdale, CA) was used. Winspec (Princeton) software was employed.

## RESULTS

### Experiments with liposomes

We measured the oxygen consumption and the NADH oxidation rates of peroxidase-containing liposomes either by adding a fixed amount of NADH (100–125  $\mu$ M) or by infusing 0.1 M NADH at a fixed rate to the reaction mixture containing liposomes. In the first case an appreciable oxygen consumption and NADH oxidation rate was only obtained if melatonin (at a concentration of 200  $\mu$ M) was also present. If melatonin was replaced by 4-hydroxybenzoic acid, no stimulation in NADH oxidation was observed. These observations indicate that the peroxidase is shielded from NADH in the solution, as both melatonin and 4-hydroxybenzoic acid are activators of the PO reaction (Olsen et al., 2001; Kummer et al., 1997; Hauser and Olsen, 1998). However, unlike melatonin, which is uncharged at pH 5.1, 4-hydroxybenzoic acid is a polar molecule with a net negative charge under the present experimental conditions.

The latter could prevent 4-hydroxybenzoic acid from diffusing across the liposomal membrane and thus inducing an acceleration in the PO reaction. Consequently, our results suggest that peroxidase is shielded from NADH in the solution by a hydrophobic barrier.

Next we investigated whether the peroxidase-containing liposomes could catalyze an oscillating PO reaction in the presence of melatonin. Fig. 1 shows a time series of the recorded absorbance changes at 360 nm and 418 nm plus the oxygen concentration when NADH is infused into a reaction mixture containing liposomes and melatonin. The absorbance changes at the two wavelengths are characteristic for NADH and peroxidase compound III, respectively. We note that the reaction oscillates, although the oscillations are strongly damped. Using an extinction coefficient for compound III at 418 nm of  $1.16 \times 10^5 \text{ M}^{-1} \text{ cm}^{-1}$  (Olsen et al., 2001), we can estimate a concentration of peroxidase in the suspension of 84 nM. This corresponds to a concentration of peroxidase in the liposome of 20  $\mu\text{M}$  as expected if peroxidase is evenly distributed between the external solution and the liposome aqueous fraction after the preparation of the liposomes.

Thus, our experiments suggest that in the presence of melatonin, horseradish peroxidase can catalyze an oscillating PO reaction even though the enzyme and one of its substrates (NADH) are located in different compartments separated by a lipid membrane.

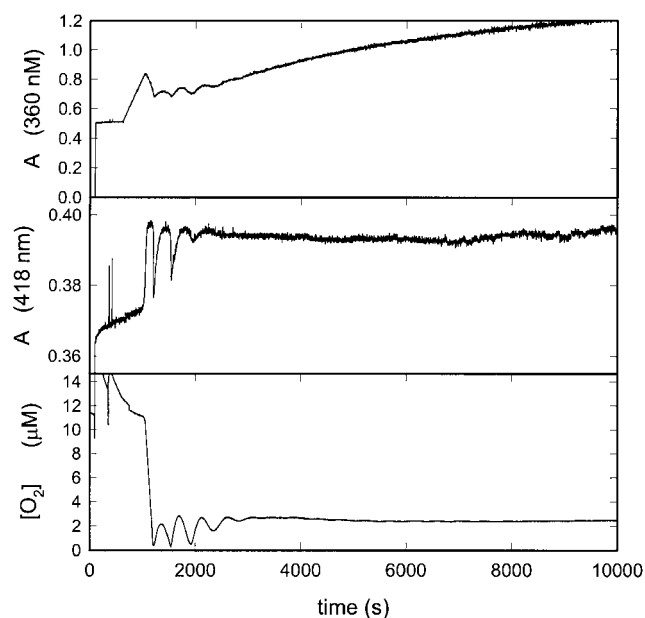


FIGURE 1 Time series of the absorbance changes at 360 nm and 418 nm plus the oxygen concentration in the peroxidase-oxidase reaction catalyzed by peroxidase-containing liposomes. The reaction mixture contained liposomes corresponding to 0.25 mM phosphatidylcholine. Other experimental conditions as described in the experimental section.

## Construction of the model

In the construction of a model for a myeloperoxidase-catalyzed PO reaction in neutrophils, one has to consider that the enzyme and one of its substrates (NADPH) are not located in the same compartment. Although NADPH is formed in the cytoplasm, the enzyme is situated either in the azurophil granules or in the phagosome. In the previous section we showed that it is possible for peroxidase to catalyze the PO reaction even when the substrate NADH and the enzyme are separated by a lipid membrane, provided that melatonin (or another nonpolar activator of peroxidase) is also present. Thus, we break our model of the PO reaction in neutrophils up into reactions that can occur in the cytosol and those that occur in the phagosome. Most of the reactions are well-documented and the *in vitro* rate constants are known (see Scheeline et al., 1997, for a review). The reactions and diffusion terms are all listed in Table 1 and the equation numbers listed below all refer to the numbers in the table.

### Reactions occurring in the cytoplasm

These include first the (very) slow autooxidation of NADPH:



The reaction is slow at pH around 7, but it may be catalyzed by a number of organic substances, e.g., methylene blue (Sevcik and Dunford, 1991). Here the reaction is modeled as a second order reaction with a very low rate constant (of the order of  $1 \text{ M}^{-1} \text{ s}^{-1}$ ).

Another reaction likely to take place in the cytosol is the reduction of molecular oxygen by the NADP<sup>•</sup> radical:

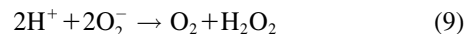


The radical NADP<sup>•</sup> is in turn regenerated in the reaction:

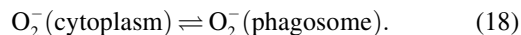


where MLTH and MLT<sup>•</sup> indicate melatonin and its free radical, respectively. The melatonin radical is formed in the reactions of melatonin with peroxidase compound I and compound II, respectively (see below).

Superoxide ( $\text{O}_2^{\bullet -}$ ) formed in reaction (8) either disproportionates:



or it diffuses from the cytoplasm into the phagosome:



As for the disproportionation of superoxide, we have assumed second order kinetics, but we have also set the second order rate constant more than 50 times as high as it should be. This is done to account for the superoxide dismutase activity in the cytoplasm. As for the diffusion of superoxide from cytoplasm to phagosome the rate is probably extremely slow. We consider the rate of this process to be essentially zero in our simulations.

**TABLE 1** Reactions and rate constants of the model of neutrophilic production of reactive oxygen species

Reaction	Rate expression ( $R_i$ )	Rate constant
Reactions occurring in phagosome:		
1. $\text{H}_2\text{O}_2 + \text{per}^{3+} \xrightleftharpoons[k_{-1}]{k_1} \text{coI}$	$k_1[\text{H}_2\text{O}_2]_p[\text{per}^{3+}]_p - k_{-1}[\text{coI}]_p$	$k_1 = 5.0 \times 10^7 \text{ M}^{-1} \text{ s}^{-1}$ $k_{-1} = 58 \text{ s}^{-1}$
2. $\text{coI} + \text{MLTH} \xrightarrow{k_2} \text{coII} + \text{MLT}^\cdot$	$k_2[\text{coI}]_p[\text{MLTH}]_p$	$k_2 = 1.0 \times 10^7 \text{ M}^{-1} \text{ s}^{-1}$
3. $\text{coII} + \text{MLTH} \xrightarrow{k_3} \text{per}^{3+} + \text{MLT}^\cdot$	$k_3[\text{coII}]_p[\text{MLTH}]_p$	$k_3 = 4.0 \times 10^3 \text{ M}^{-1} \text{ s}^{-1}$
4. $\text{per}^{3+} + \text{O}_2^- \xrightarrow{k_4} \text{coIII}$	$k_4[\text{per}^{3+}]_p[\text{O}_2^-]_p$	$k_4 = 2.0 \times 10^7 \text{ M}^{-1} \text{ s}^{-1}$
5. $2\text{H}^+ + 2\text{O}_2^- \xrightarrow{k_5} \text{H}_2\text{O}_2 + \text{O}_2$	$k_5[\text{O}_2^-]_p^2$	$k_5 = 1.0 \times 10^7 \text{ M}^{-1} \text{ s}^{-1}$
6. $\text{coIII} + \text{O}_2^- \xrightarrow{k_6} \text{coI} + \text{O}_2$	$k_6[\text{coIII}]_p[\text{O}_2^-]_p$	$k_6 = 1.0 \times 10^5 \text{ M}^{-1} \text{ s}^{-1}$
Reactions occurring in cytoplasm:		
7. $\text{NADPH} + \text{O}_2 \xrightarrow{k_7} \text{NADP}^\cdot + \text{H}_2\text{O}_2$	$k_7[\text{NADPH}]_c[\text{O}_2]_c$	$k_7 = 1 \text{ M}^{-1} \text{ s}^{-1}$
8. $\text{NADP}^\cdot + \text{O}_2 \xrightarrow{k_8} \text{NADP}^+ + \text{O}_2^-$	$k_8[\text{NADP}^\cdot]_c[\text{O}_2]_c$	$k_8 = 5.0 \times 10^7 \text{ M}^{-1} \text{ s}^{-1}$
9. $2\text{H}^+ + 2\text{O}_2^- \xrightarrow{k_9} \text{H}_2\text{O}_2 + \text{O}_2$	$k_9[\text{O}_2^-]_c^2$	$k_9 = 5.0 \times 10^8 \text{ M}^{-1} \text{ s}^{-1}$
10. $\text{MLT}^\cdot + \text{NADPH} \xrightarrow{k_{10}} \text{MLTH} + \text{NADP}^\cdot$	$k_{10}[\text{MLT}^\cdot]_c[\text{NADPH}]_c$	$k_{10} = 1.0 \times 10^7 \text{ M}^{-1} \text{ s}^{-1}$
11. $2\text{NADP}^\cdot \xrightarrow{k_{11}} (\text{NADP})_2$	$k_{11}[\text{NADP}^\cdot]_c^2$	$k_{11} = 6.0 \times 10^7 \text{ M}^{-1} \text{ s}^{-1}$
12. $\xrightarrow{k_{12}} \text{NADPH}$	$k_{12}$	$k_{12} = 22 - 35 \mu\text{M s}^{-1}$
13. $\xrightarrow[k_{-13}]{k_{13}} \text{O}_2(\text{cytoplasm})$	$k_{13} - k_{-13}[\text{O}_2]_c$	$k_{13} = 12.5 \mu\text{M s}^{-1}$ $k_{-13} = 4.5 \times 10^{-2} \text{ s}^{-1}$
Diffusion terms:		
14. $\text{O}_2(\text{phagosome}) \xrightleftharpoons[k_{14}]{k_{14}} \text{O}_2(\text{cytoplasm})$	$k_{14}([\text{O}_2]_p - [\text{O}_2]_c)$	$k_{14} = 30 \text{ s}^{-1}$
15. $\text{H}_2\text{O}_2(\text{phagosome}) \xrightleftharpoons[k_{15}]{k_{15}} \text{H}_2\text{O}_2(\text{cytoplasm})$	$k_{15}([\text{H}_2\text{O}_2]_p - [\text{H}_2\text{O}_2]_c)$	$k_{15} = 30 \text{ s}^{-1}$
16. $\text{MLTH}(\text{phagosome}) \xrightleftharpoons[k_{16}]{k_{16}} \text{MLTH}(\text{cytoplasm})$	$k_{16}([\text{MLTH}]_p - [\text{MLTH}]_c)$	$k_{16} = 10 \text{ s}^{-1}$
17. $\text{MLT}^\cdot(\text{phagosome}) \xrightleftharpoons[k_{17}]{k_{17}} \text{MLT}^\cdot(\text{cytoplasm})$	$k_{17}([\text{MLT}^\cdot]_p - [\text{MLT}^\cdot]_c)$	$k_{17} = 10 \text{ s}^{-1}$
18. $\text{O}_2^-(\text{phagosome}) \xrightleftharpoons[k_{18}]{k_{18}} \text{O}_2^-(\text{cytoplasm})$	$k_{18}([\text{O}_2^-]_p - [\text{O}_2^-]_c)$	$k_{18} = < 0.01 \text{ s}^{-1}$
NADPH oxidase:		
19. $\text{NADPH}(\text{cytoplasm}) + 2\text{O}_2(\text{phagosome}) \rightarrow \text{NADP}^+(\text{cytoplasm}) + 2\text{O}_2^-(\text{phagosome})$	$\frac{V\alpha(1+\alpha)}{(L+(1+\alpha)^2)} \frac{[\text{O}_2]_p}{K_O + [\text{O}_2]_p}; \quad \alpha = \frac{[\text{NADPH}]_c}{K_{\text{NADPH}}}$	$V = 288 \mu\text{M s}^{-1}$ $L = 550$ $K_O = 1.5 \mu\text{M}$ $K_{\text{NADPH}} = 60 \mu\text{M}$

We also assume that the  $\text{NADP}^\cdot$  radical dismutates to form a  $(\text{NADP})_2$  dimer (reaction (11)). Even though the rate constant for this reaction is fairly high, the actual rate of  $(\text{NADP})_2$  formation is low because the concentration of the radical is always very low. We have not included any oxidation of the dimer to  $\text{NADP}^+$ . Some enzymes such as peroxidase are able to use  $(\text{NADP})_2$  as a substrate (Kirkor and Scheeline, 2000).

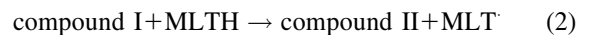
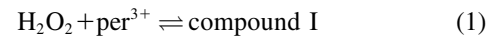
NADPH production is assumed to come exclusively from the hexose monophosphate shunt (Henderson and Chappell, 1996). In the absence of any further knowledge about the dynamics of this reaction pathway, we assume that NADPH production is constant (reaction (12)). The entry of  $\text{O}_2$  from the neighboring tissue into the cytoplasm of the neutrophil is considered to be due to simple diffusion:

$$\rightleftharpoons \text{O}_2(\text{cytoplasm}). \quad (13)$$

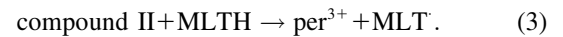
Here we have taken a very conservative view on the maximum rate of oxygen diffusion into the cell ( $\sim 0.75 \text{ mM}$  per minute), which is small compared to the rate of oxygen consumption in cardiac tissue (McCord, 2000).

#### Reactions occurring in the phagosome

These include the classical peroxidase cycle:

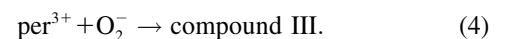


and



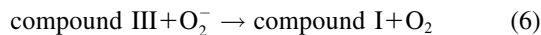
Note that reaction (1), in contrast to the corresponding reaction involving horseradish peroxidase, is reversible (Furtmüller et al., 2000). The rate constants for reactions (1),  $k_1$  and  $k_{-1}$  listed in Table 1 are taken from Furtmüller et al. (2000), whereas the rate constants  $k_2$  and  $k_3$  are taken from Allegra et al. (2001).

The free ferric enzyme may form compound III by reaction with superoxide:



In the absence of any reported rate constant for

myeloperoxidase we have used the corresponding rate constant  $k_4$  measured for horseradish peroxidase (Scheeline et al., 1997). In homogeneous solution there is an alternative way of forming compound III through reduction of ferric peroxidase to ferrous peroxidase by the NAD(P)<sup>•</sup> radical and subsequent oxygenation of ferrous peroxidase (Bronnikova et al., 1995). However, as the NAD<sup>•</sup> radical is probably not able to enter the phagosome, these reactions are not included in the present model. As in the cytosol superoxide may disproportionate (reaction (5)), but in this case the reaction is not considered to be catalyzed by superoxide dismutase. In most detailed models compound III is reduced to compound I through reaction with the NAD(P)<sup>•</sup> radical. For the same reason as given above for the formation of ferrous peroxidase this reaction is probably not occurring in the phagosome. Instead we have included the reaction:



as recently proposed in Baker et al. (2000). In the absence of detailed knowledge about the magnitude of  $k_6$ , we have chosen a reasonably low value for this reaction.

#### Diffusion terms

The present model assumes exchange of electrons between components in two different cellular compartments. The following species must be able to permeate the lipid membrane, either by simple diffusion or by mediated transport: oxygen and hydrogen peroxide, melatonin and its corresponding free radical, and superoxide. The latter molecule will probably cross the lipid membrane as the uncharged protonated form ( $\text{HO}_2$ ). However, we cannot exclude that the phagosome membrane, like the plasma membrane, contains an anion channel through which the unprotonated form can enter the phagosome. In any case the rate of diffusion of  $\text{O}_2^-$  across the phagosome membrane will be considered to be very slow. The diffusional terms are computed from Fick's law of diffusion:

$$J_X = P_X([X]_p - [X]_c), \quad (6)$$

where  $J_X$  is the flux (mol/unit area) of substance  $X$ , and  $P_X$  is the permeability coefficient of that substance. The permeability coefficients are converted to pseudo first order rate constants and the magnitude of these constants are calculated from the equations:

$$k_X = \frac{3P_X}{r}, \quad (6)$$

where  $r$  is the radius of the phagosome. Because  $r$  is of the order of 0.2–0.5  $\mu\text{m}$ , and the permeability coefficients are of the order of  $10^{-7}$  cm/s to  $10^{-3}$  cm/s, we can compute first order coefficients for the reactions (14)–(18) of  $0.006 \text{ s}^{-1}$  to  $150 \text{ s}^{-1}$ . The permeability coefficient of  $\text{H}_2\text{O}_2$  for the plasma membrane of *Chara corallina* was estimated as  $3.6 \times 10^{-4}$  cm/s (Henzler and Steudle, 2000) suggesting a first order constant of 20–50  $\text{s}^{-1}$ . We can easily assume that

the permeability coefficient of  $\text{O}_2$  is no less than that. As for the permeability coefficients of melatonin and its free radical form, we have assumed values around  $10^{-4}$  cm/s resulting in pseudo first order constants of the order of  $10 \text{ s}^{-1}$ . It was previously shown that melatonin can easily cross lipid bilayers, suggesting a high permeability coefficient (Costa et al., 1995).

#### NADPH oxidase

Upon activation of neutrophils, this membrane-associated multisubunit enzyme is recruited and assembled in the phagosome membrane (Hampton et al., 1998; Henderson and Chappell, 1996; Jones et al., 2000). The function of the enzyme is to produce superoxide radicals in the phagosome. The electrons needed for the reduction of oxygen come from NADPH, which again is formed by the hexose monophosphate shunt. The stoichiometry of the reaction is:



NADPH oxidase is a very complex enzyme, the activity of which requires the involvement of at least two G-proteins (Jones et al., 2000). These proteins act as molecular switches that turn the enzyme's activity on and off when they alternate between binding GTP in the active form and GDP in the inactive form. Thus the activity of NADPH oxidase undoubtedly has a very complex kinetics with respect to its two substrates, NADPH and  $\text{O}_2$ . Here we have taken a simple nonlinear dependence of the enzyme kinetics of NADPH oxidase, namely that the enzyme shows cooperativeness with respect to the binding of NADPH and simple Michaelis-Menten behavior with respect to  $\text{O}_2$  (see Table 1). The dissociation constant for the binding of NADPH is set to 60  $\mu\text{M}$  (Henderson and Chappell, 1996), and the Michaelis constant for oxygen is assumed to be around 1.5  $\mu\text{M}$ . The maximal rate of the oxidase was estimated at 288  $\mu\text{M/s}$  in accordance with values of around 10 nmol/ $10^6$  cells per 10 min reported in Levy et al. (1994). However, it should be emphasized that the exact kinetic expression for NADPH oxidase and the constants assumed for the binding of its substrates as well as its maximal turnover number are not critical for the behavior of the model.

The differential equations corresponding to the model presented in Table 1 are listed in Table 2. The concentration changes in the phagosome are indicated with a subscript  $p$  whereas the concentration changes in the cytosol are indicated with a subscript  $c$ . The factor  $f$  refers to the fractional volume of the phagosome over the cytosol volume and is set to 1:10 in all simulations. However, both higher and lower values of  $f$  yield oscillating solutions of the equations in Table 2.

#### Simulation results

In the absence of NADPH oxidase activity, the simulations of the differential equations in Table 2 yield only damped

**TABLE 2** Differential equations

Phagosome:

$$d[\text{per}^{3+}]_p/dt = -R_1 + R_3 - R_4$$

$$d[\text{coI}]_p/dt = R_1 - R_2 + R_6$$

$$d[\text{coII}]_p/dt = R_2 - R_3$$

$$d[\text{coIII}]_p/dt = R_4 - R_6$$

$$d[\text{H}_2\text{O}_2]_p/dt = -R_1 + R_5 - R_{15}$$

$$d[\text{O}_2^-]_p/dt = -R_4 - 2R_5 - R_6 - R_{18} + 2R_{19}$$

$$d[\text{O}_2]_p/dt = R_5 + R_6 - R_{14} - 2R_{19}$$

$$d[\text{MLTH}]_p/dt = -R_2 - R_3 - R_{16}$$

$$d[\text{MLT}]_p/dt = R_2 + R_3 - R_{17}$$

Cytoplasm:

$$d[\text{NADPH}]_c/dt = -R_7 - R_{10} + R_{12} - R_{19}$$

$$d[\text{NADP}^+]_c/dt = -R_8 + R_{10} - 2R_{11}$$

$$d[\text{H}_2\text{O}_2]_c/dt = R_7 + R_9 + fR_{15}$$

$$d[\text{O}_2^-]_c/dt = R_8 - 2R_9 + fR_{18}$$

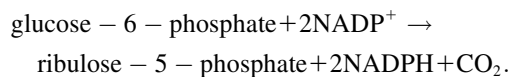
$$d[\text{O}_2]_c/dt = -R_7 - R_8 + R_9 + R_{13} + fR_{14}$$

$$d[\text{MLTH}]_c/dt = R_{10} + fR_{16}$$

$$d[\text{MLT}]_c/dt = -R_{10} + fR_{17}$$

oscillations, very much like the experimental time series shown in Fig. 1. Sustained oscillations can be obtained if the permeability coefficient for superoxide is increased to unrealistic high values, corresponding to values of  $k_{18} > 1 \text{ s}^{-1}$ . However, introducing NADPH oxidase activity into the model results in sustained oscillations. An example is shown in Fig. 2. Here we have assumed a total concentration of myeloperoxidase in the phagosome of around  $300 \mu\text{M}$ . This is a lower boundary estimated from the reported value of an average cell concentration of around  $30 \mu\text{M}$  if the enzyme was uniformly distributed in the cell (Sørensen and Borregaard, 1999). The melatonin free radical also oscillates with the same frequency as the oscillations shown in Fig. 2.

When a neutrophil is activated, the hexose monophosphate shunt starts to produce NADPH through oxidation of glucose-6-phosphate to ribulose-5-phosphate:



The NADPH produced is mainly used for the reduction of oxygen to reactive oxygen species, i.e., hydrogen peroxide, superoxide, and hydroxyl radical. We have simulated the flux of production of NADPH as a single constant,  $k_{12}$ , the value of which is increasing as the neutrophils are activated. Fig. 3 shows the effect on the oscillation period when  $k_{12}$  is increased from 23.5 to  $34 \mu\text{M/s}$ . Outside this interval the system displays only steady-state behavior. We note that as  $k_{12}$  is increased, the oscillation period decreases from around 200 s to between 15 and 20 s. These periods are in the same range as those observed experimentally in migrating neutrophils (Amit et al., 1999).

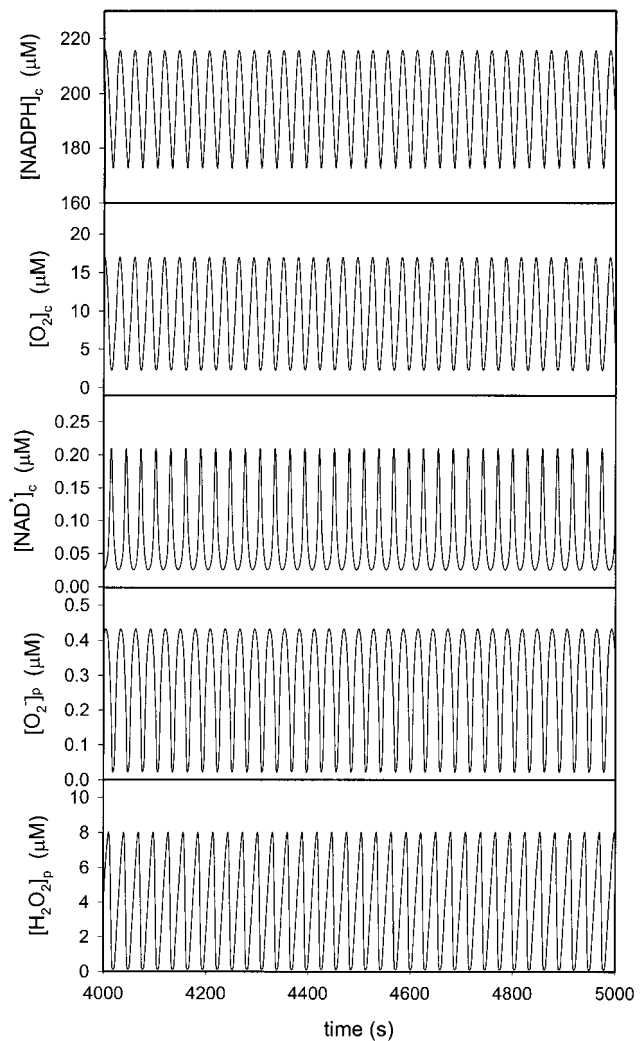


**FIGURE 2** Simulated time series of the concentrations of cytosolic NADPH, oxygen, and NADP<sup>+</sup> radical as well as superoxide and hydrogen peroxide in the phagosome. The simulations were made using the model listed in Table 1 and Table 2. The flux of formation of NADPH ( $k_{12}$ ) was set at  $30 \mu\text{M/s}$ . Other parameters as listed in Table 1. The initial concentrations of ferric peroxidase and melatonin were both  $300 \mu\text{M}$ . The initial concentration of all other substances was zero.

The oscillation period is less sensitive to concentrations of peroxidase and melatonin. Fig. 4 shows the change in oscillation period when the concentration of peroxidase is increased from  $200 \mu\text{M}$  to  $800 \mu\text{M}$  and the concentration of melatonin is increased from  $200 \mu\text{M}$  to  $1000 \mu\text{M}$ . At low initial concentrations of the enzyme, an increase in the initial concentration of melatonin is accompanied by a dramatic increase in oscillation amplitude (Fig. 5).

As mentioned above, sustained oscillations in our model system cannot be accomplished without some NADPH oxidase activity. The amount of NADPH oxidase activity in the model has very little effect on the oscillation amplitude or the period. However, the higher the maximum NADPH

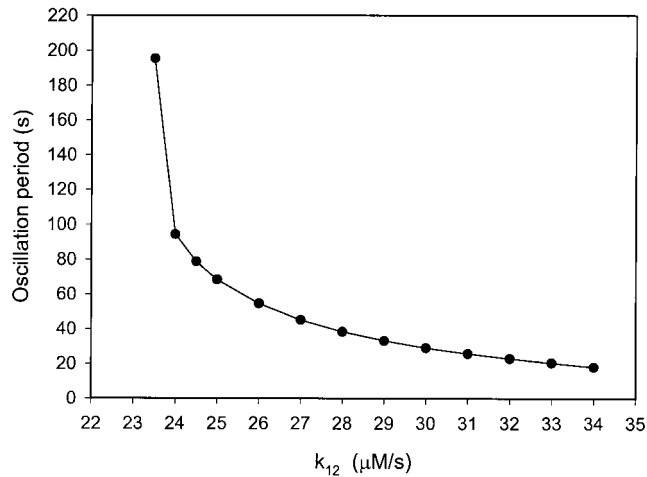
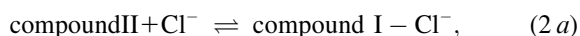
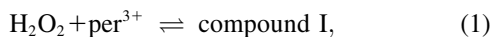


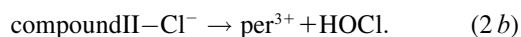
FIGURE 3 Effect of the rate of NADPH influx ( $k_{12}$ ) on the oscillation period. Parameters and initial conditions as in Fig. 2.

oxidase activity, the broader is the parameter regions where sustained oscillations are observed. Thus, the formation of superoxide through NADPH oxidation is not only crucial in the release of superoxide in the phagosome. It is also essential for the periodic formation of this radical. Our simulations showed large periodic fluctuations in the activity of NADPH oxidase (Fig. 6). On the other hand, a system consisting of NADPH oxidase alone, with the nonlinear properties listed in Table 1, cannot give rise to oscillations. Thus it is the cooperation of peroxidase and NADPH oxidase that secures the periodic activity. Note that the amplitude of the NADPH oxidase activity oscillations in Fig. 6 is considerably smaller than the maximum velocity of that enzyme  $V = 288 \mu\text{M s}^{-1}$  (Table 1). We were able to obtain oscillations with considerably smaller values of  $V$ . This implies that in order to abolish oscillatory dynamics in this system, one would have to inhibit NADPH oxidase by more than 75%.

Previously, it was postulated that the main function of myeloperoxidase in the phagosome is to produce hypochlorous acid from chloride according to the following reactions (Furtmüller et al., 2000):



and



Obviously, the reactions 2 *a* and 2 *b* compete with reactions 2 and 3 of our model. Furthermore, it was shown (Hampton et al., 1998) that a substantial fraction of the  $\text{H}_2\text{O}_2$  formed in the phagosome is converted into HOCl. In order to check if these reactions have a profound impact on the modeling results, we included them in the model and studied the resulting simulations. Using the experimentally deter-

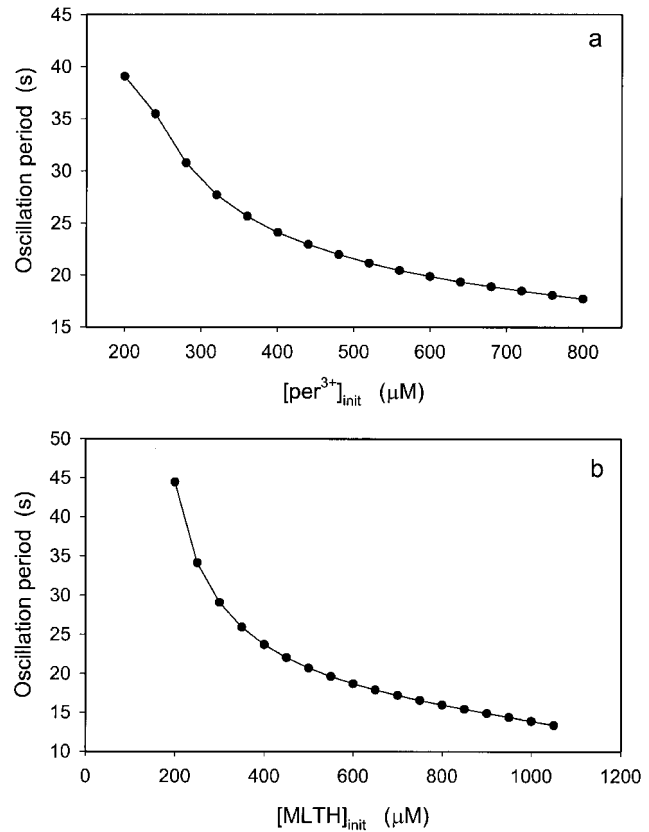


FIGURE 4 Effect of the initial concentrations of (a) ferric peroxidase ( $\text{per}^{3+}$ ) and (b) melatonin on the oscillation period. The NADPH influx rate was  $30 \mu\text{M/s}$ . In (a) the initial concentration of melatonin was  $300 \mu\text{M}$ , whereas in (b) the initial concentration of ferric peroxidase was  $300 \mu\text{M}$ . Other parameters and initial conditions as in Fig. 2.

mined kinetic rate constants for reactions 2 *a* and 2 *b* (Furtmüller et al., 2000), we observed that including these reactions in the model does indeed inhibit the oscillatory behavior. However, with the kinetic parameters used, almost 100% of the oxygen taken up by the neutrophils would be incorporated into HOCl. This does not match corresponding experimental data showing that only 20–70 percent of  $\text{H}_2\text{O}_2$  is incorporated. An explanation for this could be that the parameters that were determined experimentally in vitro might be different in the in vivo system. We therefore reduced the rate constant for the forward reaction in Eq. 2 *a* to such a degree that up to 70% of the oxygen consumed in the phagosome is used for the production of HOCl. Under these circumstances, the oscillatory behavior is restored (data not shown) and the above described modeling results remain valid.

## Experiments with cells

We next sought to test certain assumptions of the model described above and its predictions based upon the

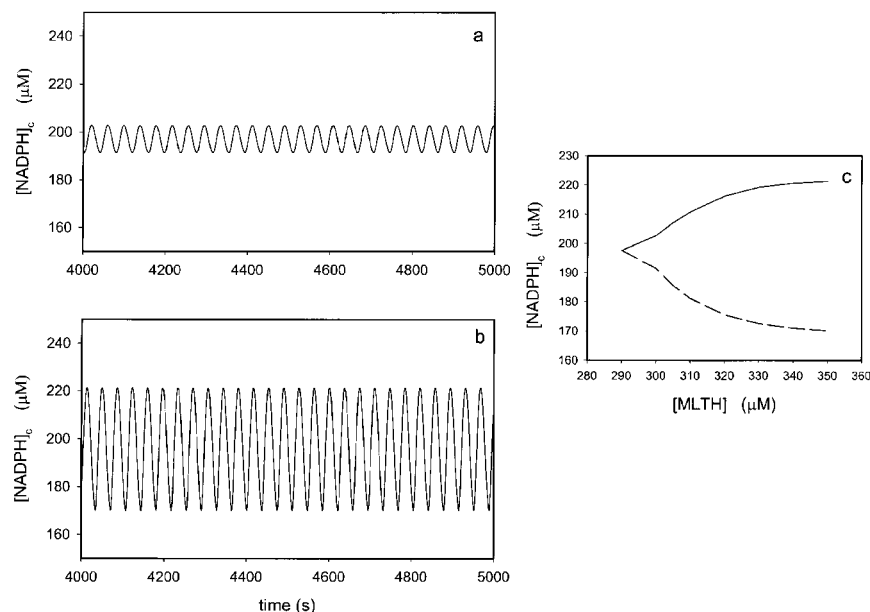


FIGURE 5 Effect of the concentration of melatonin on the oscillation amplitude. Time series of  $[NADPH]_c$  in the presence of an initial concentration of melatonin of (a)  $300 \mu M$  and (b)  $350 \mu M$ . (c) Envelope of the oscillations of NADPH plotted against the concentration of melatonin ( $[MLTH]$ ) in the cytoplasm. The NADPH influx rate was  $30 \mu M/s$  and the initial concentration of ferric peroxidase was  $200 \mu M$ . Other conditions as in Fig. 2.

simulation results. The model replicates key features of an activated neutrophil, such as the reliance on the hexose monophosphate shunt (HMS), activation of the NADPH oxidase, and mobilization of myeloperoxidase. In the first series of cell experiments, we sought to establish the contribution of the HMS in NAD(P)H oscillations. To accomplish this goal, we employed the reagent 6-aminonicotinamide (6-AN), which is known to block the activity of glucose-6-phosphate dehydrogenase and 6-phosphogluconate dehydrogenase; both of these enzymes are specific for the HMS (White et al., 1978).

Adherent neutrophils were incubated in the presence or

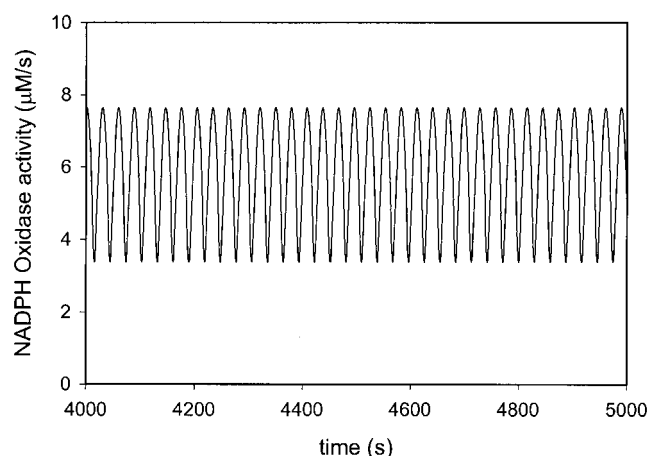


FIGURE 6 Simulated changes of activity of NADPH oxidase (reaction (19) in Table 1). The flux of formation of NADPH ( $k_{12}$ ) was set at  $30 \mu M/s$ . Other parameters as in Table 1. The initial concentrations of ferric peroxidase and melatonin were both  $300 \mu M$ . The initial concentration of all other substances was zero.

absence of 6-AN at  $10 \text{ mM}$  for  $30 \text{ min}$  at  $37^\circ C$ ; previous studies have shown that these conditions effectively block neutrophil activation and the respiratory burst (e.g., Bender and Van Epps, 1985). In the absence of added reagents, NAD(P)H oscillations with a period of  $20 \text{ s}$  are observed. However, the activating chemotactic peptide *N*-formyl-methionyl-leucyl-phenylalanine (FMLP,  $100 \text{ nM}$ ), which induces a vigorous respiratory burst, triggers the appearance of a  $10 \text{ s}$  period in NAD(P)H oscillations (Fig. 7), which has been previously observed (Petty, 2001; Amit et al., 1999). The reagent 6-AN has no effect on the  $20 \text{ s}$  oscillations, but eliminates the acquisition of the  $10 \text{ s}$  NAD(P)H oscillation in the presence of FMLP (Fig. 7). Parallel results were obtained using the somewhat less specific reagent dexamethasone (Fig. 7), which also inhibits glucose-6-phosphate dehydrogenase (Whitcomb and Schwartz, 1985; Rom and Harkin, 1991; Mohan and Jacobson, 1993). As previously suggested using various neutrophil activating substances (Petty, 2001; Amit et al., 1999), these findings indicate that the  $20 \text{ s}$  oscillation is associated with cell adherence/motility, but not activation or utilization of the HMS, whereas the  $10 \text{ s}$  oscillation is only found in activated cells and draws upon the HMS.

One of the key findings in the simulation studies was that the NADPH oxidase and myeloperoxidase cooperate in the development of stable oscillations. To test this prediction, we employed the reagent diphenyleneiodonium (DPI), which inhibits the NADPH oxidase (Cross and Jones, 1986). Cells were incubated with DPI at various concentrations for  $45 \text{ min}$  at  $37^\circ C$ . In the range of  $0\text{--}20 \mu g/ml$  DPI had no effect on NAD(P)H oscillations (Fig. 8 A). At a higher dose of  $25\text{--}35 \mu g/ml$  DPI, FMLP had no effect on NAD(P)H oscillations of neutrophils (Fig. 8 B). No NAD(P)H oscillations were observed at doses above  $40 \mu g/ml$  DPI (Fig. 8 C). Under the



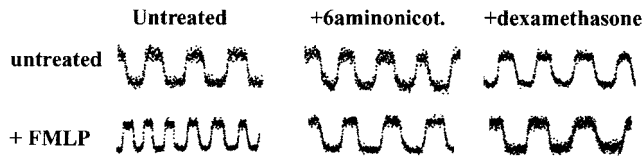


FIGURE 7 The effects of 6-aminonicotinamide and dexamethasone on NAD(P)H oscillations of polarized neutrophils. When neutrophils are exposed to 100 nM FMLP, the frequency of the NAD(P)H oscillations are approximately doubled. 6-aminonicotinamide, a reagent that specifically blocks the HMS, has no effect on untreated cells, but blocks the frequency change accompanying FMLP exposure. A similar effect was noted with the inhibitory drug dexamethasone.

conditions we have employed (adherent cells, HBSS, etc.), concentrations in the range of 100  $\mu\text{g/ml}$  appeared to be toxic to the cells. Our findings confirm the role of the NADPH oxidase in establishing the 10 s NAD(P)H oscillation period.

Our modeling studies led to the unanticipated prediction that melatonin should affect the amplitude of metabolic oscillations in activated neutrophils. We therefore studied the nature of melatonin interactions with adherent neutrophils and its effect on NAD(P)H oscillations. In the first series of experiments, we examined melatonin-neutrophil interactions. Previous studies have established that optimal enhancement of the respiratory burst occurs at roughly 50–100  $\mu\text{M}$  melatonin (Recchioni et al., 1998). Therefore, neutrophils were incubated with 50  $\mu\text{M}$  melatonin for 30 min at 37°C followed by addition of 50 nM FMLP. The oxidation of melatonin by peroxidase is accompanied by chemiluminescence via a dioxetane intermediate (Silva et al., 2000). The chemiluminescence properties of melatonin in neutrophils were examined using an imaging spectrophotometer system. The chemiluminescence spectrum was centered at  $\sim 515$  nm (Fig. 9 C). Using an intensifier and camera cooled to  $-20^\circ\text{C}$ , the chemiluminescence was imaged by accumulating data for 10 s. These images showed that FMLP-treated cells exhibited chemiluminescence within the anterior region of the cell body and lamellipodium (Fig. 9 B), which are areas rich in intracellular granules and peroxidase. When the chemiluminescence was quantitated as a function of time, it was found to oscillate (Fig. 9 D), as does hydrogen peroxide, a cofactor in its oxidation. There-

fore, melatonin undergoes chemical reactions within living human neutrophils.

We next tested the effect of melatonin on NAD(P)H oscillations of neutrophils. Incubation of neutrophils with melatonin (50  $\mu\text{M}$ ) for 30 min at 37°C had no effect on nonactivated neutrophils expressing the 20 s NAD(P)H oscillations (Fig. 10 A). In contrast, FMLP-activated neutrophils displayed enhanced NAD(P)H oscillatory amplitudes in the presence of melatonin (Fig. 10, A and D). Thus, the melatonin effect anticipated by the model (Fig. 5) is replicated in living cells (Fig. 10), but only during neutrophil activation, which, in turn, is an explicit condition of the model. In the absence of cell stimulation, 20 s oscillations and low levels of reactive oxygen metabolite (ROM) production are found for polarized cells (Fig. 10 B), as previously described (Petty, 2001; Amit et al., 1999). The level of ROM production is enhanced by activating agents such as FMLP and further enhanced by the inclusion of melatonin (Fig. 10, B, C, E, and F). This accounts for the “priming” effect of melatonin reported in the literature (Recchioni et al., 1998; Morrey et al., 1994); melatonin is incapable of initiating a respiratory burst, but is capable of enhancing ROM production in the presence of a second activating signal.

## DISCUSSION

In the present study we have developed a robust *in silico* model of cell metabolism during neutrophil activation and tested several experimentally accessible features of the model on living neutrophils. The model encompasses several essential cellular and chemical features of activated neutrophils. Key features include the activation of the NADPH oxidase, delivery of myeloperoxidase to endosomes, and activation of the HMS. The model is robust in the sense that it is consistent with previous experimental findings and successfully predicted the behavior of neutrophil metabolism in the presence of melatonin. The synergy between the *in silico* and *in vitro* methods in cell biology has enhanced greatly our understanding of the links between the dynamics of intracellular chemistry and time-varying properties of neutrophil physiology.

Previous experimental studies have shown that polarized

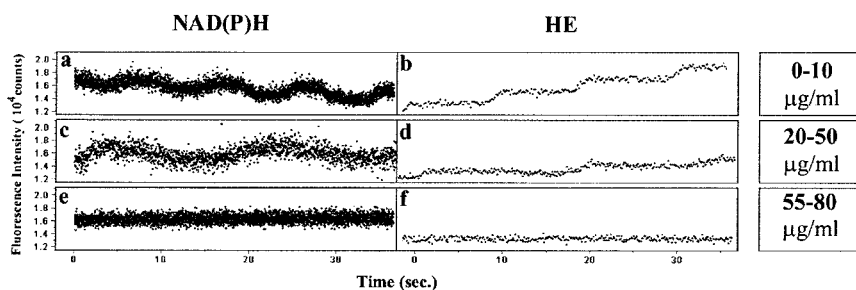


FIGURE 8 The effect of DPI on NAD(P)H oscillations (a, c, and e) and superoxide release, as judged by the conversion of hydroethidine to ethidium bromide in the cellular environment, for polarized neutrophils. Although DPI had no effect on FMLP-stimulated NAD(P)H oscillations at low doses (0–10  $\mu\text{g/ml}$ ), doses in the range of 20–50  $\mu\text{g/ml}$  DPI blocked acquisition of the  $\sim 10$  s period oscillation. Higher doses caused metabolic dynamics to disappear. Superoxide release paralleled the changes in NAD(P)H oscillations.

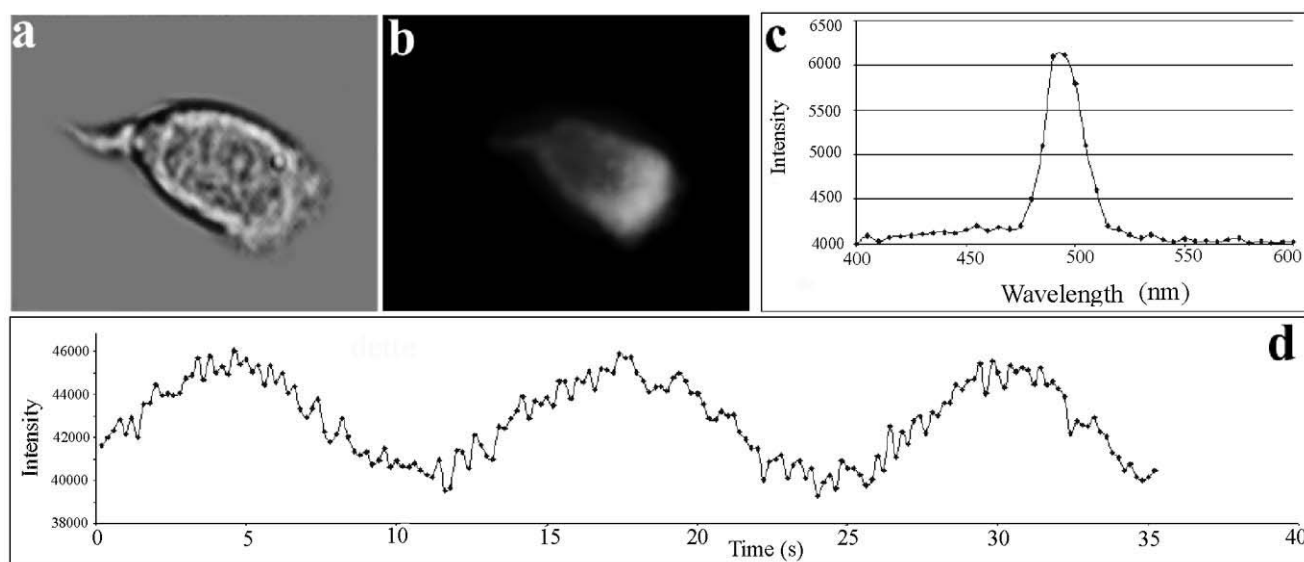


FIGURE 9 Chemiluminescence properties of melatonin-labeled neutrophils. The chemiluminescence was imaged using a cooled detector. DIC and chemiluminescence images are shown in panels *a* and *b*, respectively. The chemiluminescence spectrum is shown in panel *c*. In panel *d* the chemiluminescence intensity is plotted as a function of time, which shows oscillations in the output intensity.

neutrophils exhibit NAD(P)H oscillations with a period of  $\sim 20$  s for untreated cells and  $\sim 10$  s for activated neutrophils (Petty, 2001; Amit et al., 1999). These two distinct periods apparently correspond to two different biochemical pathways. The 20 s oscillatory period presumably reflects the glycolytic apparatus (the nonHMS, 6-AN-insensitive component (Fig. 7)) whereas the 10 s oscillation corresponds to the HMS/NADPH oxidase/myeloperoxidase-dependent (6-AN-sensitive) component of metabolism for activated neutrophils, as modeled above.

The model predicts metabolic oscillations whose period is consistent with experimental observations. The central feature of the model is the cooperation of the NADPH oxidase and myeloperoxidase. The requirement of the NADPH oxidase to stabilize the oscillatory pattern has been confirmed by inactivating the oxidase using DPI, an inhibitor of the oxidase (Cross and Jones, 1986). As predicted by the modeling results, higher concentrations of DPI blocked the 10 s oscillations. Interestingly, at a DPI dose of 25–35 mg/

ml, the 20 s oscillation was observed in the presence of FMLP. We suggest that this concentration range is associated with inhibition of the stable oscillations linked with NADPH oxidase-myeloperoxidase cooperation, but that the glycolytic pathway is not significantly affected. At higher DPI concentrations, additional metabolic pathways might be affected.

The model predicted that melatonin enhances the amplitude of NAD(P)H oscillations. The melatonin effect was subsequently tested in neutrophils. Our results showed that melatonin, indeed, enhanced the amplitude of the 10 s NAD(P)H oscillations of activated neutrophils, but had no effect on the 20 s NAD(P)H oscillations. Not only does this confirm the model described above, but it is also consistent with the association of the 10 and 20 s NAD(P)H oscillations with two distinct metabolic pathways. Thus, the model has successfully accounted for prior experimental observations and predicted the effects of DPI and melatonin on living cells.

Oscillations in NAD(P)H are accompanied by oscillations

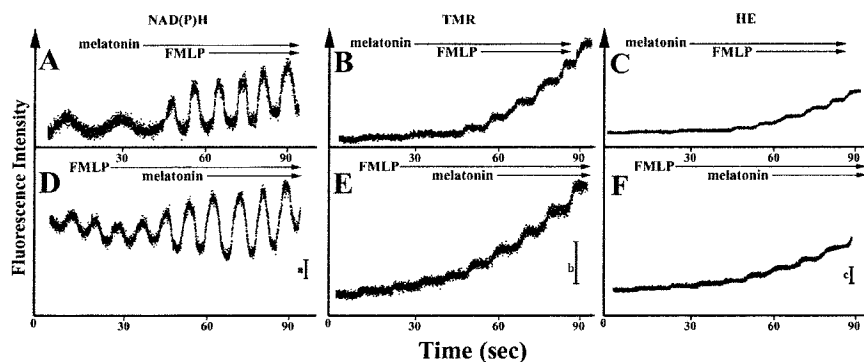


FIGURE 10 The effects of melatonin ( $50 \mu\text{M}$ ) and FMLP ( $50 \text{ nM}$ ) on NAD(P)H oscillations and oxidant release. (A) Although melatonin alone has no effect on NAD(P)H oscillations, when FMLP is added to the cells both the frequency and amplitude of the oscillations are increased. (B and C) The production of oxidants as detected by tetramethylrhodamine and EB formation are dramatically enhanced in the presence of melatonin and FMLP. (D) As noted in Fig. 7, FMLP increases the frequency of NAD(P)H oscillations. When melatonin is added, the amplitude increases. (E and F) The production of oxidants is enhanced by FMLP and further enhanced when melatonin is added.

in superoxide and hydrogen peroxide production (Fig. 2). Changes in NAD(P)H oscillation frequency or amplitude are paralleled by changes in oxidant production. The low levels of oxidant production shown above for nonactivated neutrophils displaying the 20 s oscillation have been previously observed by several laboratories (Demaurex et al., 1996; Ginis and Tauber, 1990; Kindzelskii et al., 1998). These oscillations are apparently independent of the HMS. Activation of the HMS is accompanied by higher frequency oscillations and enhanced oxidant production.

The modeling studies described above characterize the properties of activated neutrophils; hence, they do not address the 20 s NAD(P)H oscillations. Also, the modeling results do not account for the dominance of the 10 s oscillations in the presence of neutrophil activating stimuli. We believe that the disappearance of the 20 s component may be due to a greater flux of carbon through the HMS relative to glycolysis. Further analysis of the glycolytic pathway in neutrophils should provide further insights into the coupling of these two oscillators. Importantly, combined modeling/experimental studies should help explain cell-mediated damage due to high glucose levels in diabetes and the unusual metabolic changes in neutrophils during polytrauma (Oehler et al., 2000).

The effect of melatonin on activated leukocytes is interesting for several reasons. Melatonin is a pineal hormone and a biosynthetic product of leukocytes (Finocchiaro et al., 1991). It has an unexplained ability to prime neutrophils and monocytes for oxidant production, cytotoxicity, and other functions (Recchioni et al., 1998; Morrey et al., 1994). Melatonin, a priming agent, enhances oxidant production in response to activating stimuli, such as lipopolysaccharide and phorbol myristate acetate (PMA), but does not induce a response in the absence of an activating stimulus. Previous studies have demonstrated the priming of oxidant production using flow cytometric and superoxide dismutase-inhibitable cytochrome c reduction methodologies (Recchioni et al., 1998; Morrey et al., 1994). In the present study we confirm these findings using single cell fluorescence techniques and correlate this enhancement with an increase in the amplitude of NAD(P)H oscillations. Other studies have shown that activated neutrophils oxidize melatonin (Silva et al., 2000; Recchioni et al., 1998), which suggests that chemical reactions of melatonin participate in leukocyte priming.

The modeling studies also suggest a likely chemical mechanism of melatonin-induced neutrophil priming. The enhanced NADPH and oxidant oscillatory amplitudes predicted by the model and observed experimentally explain why the levels of oxidant production are higher in the presence of melatonin. Because the model is only applicable to activated neutrophils, nonactivated neutrophils are not susceptible to melatonin-mediated enhancement. This is mainly due to the fact that the model predicts that melatonin enhances the myeloperoxidase catalyzed oxidation of

NAD(P)H. Myeloperoxidase is only released from granules upon activation of the neutrophils. Therefore, as a priming agent, it cannot enhance oxidant production in the absence of an activating stimulus.

The ability of melatonin to enhance oxidant production by leukocytes may seem paradoxical due to its ability to scavenge reactive oxygen and nitrogen species (Matuszak et al., 1997; Zhang et al., 1998). In a physiological context, however, these contrasting abilities may be advantageous. In the local environment of a neutrophil, melatonin would promote higher oxidant levels, thereby enhancing host defense. However, at some distance from a neutrophil, melatonin's ability to act as a scavenger may minimize collateral damage to healthy host tissues.

Enhanced amplitudes of NAD(P)H and superoxide oscillations have also been observed in neutrophils in response to the biological factors interferon- $\gamma$  (Adachi et al., 1999; Rosenspire et al., 2000) and interleukin-12 (unpublished) and other stimulatory conditions provided by PMA and electric fields (Kindzelskii and Petty, 2000). Not surprisingly, at appropriate doses interferon- $\gamma$  and PMA prime cells for oxidant production (Tyagi et al., 1988; Berton et al., 1986). Interferon- $\gamma$  and interleukin-12 transmit intracellular signals via calcium (Aas et al., 1998; Aas et al., 1999; Collison et al., 1998). Furthermore, PMA acts on the calcium signaling circuitry (Tauber, 1987). Thus, similar metabolic responses can be achieved by several calcium-related stimuli. One possibility to account for this is that calcium signals may promote mixing of the NADPH oxidase and myeloperoxidase into the same compartment via membrane fusion whereas melatonin may promote electron trafficking in the absence of vesicle fusion. Alternatively, because interferon- $\gamma$  induces the synthesis of melatonin (Finocchiaro et al., 1988), it is possible that melatonin is the mediator responsible for the interferon- $\gamma$ -mediated enhancement of NAD(P)H and oxidant oscillations. Because melatonin is relatively mobile, one might discriminate between these two possibilities by mixing interferon- $\gamma$ -primed cells with untreated cells then assaying for amplitude modulation in the untreated cells.

One problem with the conventional reductionist approach to rational drug development is that a specific compound designed to affect a specific enzyme often has just the opposite of the desired effect at the cellular level or in patient care. A goal of biocomplexity research is the identification of important interactions, pathways, feedback loops, etc. such that biochemical pathways and living tissues can be intelligently perturbed. Due to their relative simplicity and profound clinical importance, neutrophils are an excellent system for computational analysis. Our model of neutrophil activation was found to be consistent with earlier experimental findings and successfully predicted the novel experimental results described above (Figs. 7–10). The apparent resolution of the mechanism of melatonin-mediated neutrophil priming is a useful example of the importance of

computer simulations in biology. The interplay of in silico and in vitro research will have a major impact on modern biology and medicine.

The authors thank the Klaus Tschira Foundation for financial support of this project. In addition, one of the authors (L.F.O.) acknowledges additional support from the Danish Natural Science Research Council, the Novo Nordisk Foundation, and the Carlsberg Foundation. We also acknowledge support from the National Institutes of Health (grants AI27409 and CA74120).

Simulations were performed using the Rosenbrock routine for the numerical solution of stiff differential equations. The software used was MADONNA (University of California, Berkeley, CA).

## REFERENCES

- Aas, V., K. Larsen, and J. G. Iversen. 1998. IFN-gamma induces calcium entry in human neutrophils. *J. Interferon Cytokine Res.* 18:197–205.
- Aas, V., K. Larsen, and L. G. Iversen. 1999. Interferon-gamma elicits a G-protein-dependent  $\text{Ca}^{2+}$  signal in human neutrophils after depletion of intracellular  $\text{Ca}^{2+}$  stores. *Cell. Sign.* 11:101–110.
- Adachi, Y., A. L. Kindzelskii, N. Ohno, T. Yadomae, and H. R. Petty. 1999. Amplitude and frequency modulation of metabolic signals in leukocytes: synergistic role in interferon- $\gamma$  in interleukin-6 and interleukin-2-mediated cell activation. *J. Immunol.* 163:4367–4374.
- Allegra, M., P. G. Furtmüller, G. Regelsberger, M. L. Turco-Liveri, L. Tesoriere, M. Peretti, M. A. Livrea, and C. Obinger. 2001. Mechanism of the reaction of melatonin with human myeloperoxidase. *Biochem. Biophys. Res. Commun.* 282:380–386.
- Amit, A., A. L. Kindzelskii, J. Zani, J. N. Jarvis, and H. R. Petty. 1999. Complement deposition on immune complexes reduces the frequencies of metabolic, proteolytic, and superoxide oscillations of migrating neutrophils. *Cell. Immunol.* 194:47–53.
- Baker, C. J., K. Deahl, J. Domek, and E. W. Orlandi. 2000. Scavenging of  $\text{H}_2\text{O}_2$  and production of oxygen by horseradish peroxidase. *Arch. Biochem. Biophys.* 382:232–237.
- Bender, J. G., and D. E. Van Epps. 1985. Inhibition of human neutrophil function by 6-aminocotinamide: the role of the hexose monophosphate shunt in cell activation. *Immunopharm.* 10:191–199.
- Berton, G., L. Zeni, M. A. Cassatella, and F. Rossi. 1986. Gamma interferon is able to enhance the oxidative metabolism of human neutrophils. *Biochem. Biophys. Res. Commun.* 138:1276–1282.
- Bronnikova, T. V., V. R. Fed'kina, W. M. Schaffer, and L. F. Olsen. 1995. Period-doubling bifurcations and chaos in a detailed model of the peroxidase-oxidase reaction. *J. Phys. Chem.* 99:9309–9312.
- Collison, K., S. Saleh, R. Parhar, B. Meyer, A. Kwaasi, K. Al-Hussein, S. Al-Sedairy, and F. Al-Mohanna. 1998. Evidence that IL-12-activated  $\text{Ca}^{2+}$  and tyrosine signaling pathways in human neutrophils. *J. Immunol.* 161:3737–3745.
- Costa, E. J. X., R. H. Lopes, and M. T. Lamy-Freund. 1995. Permeability of pure lipid bilayers to melatonin. *J. Pineal Res.* 19:123–126.
- Cross, A. R., and O. T. G. Jones. 1986. The effect of the inhibitor diphenylene iodonium on the superoxide-generating system of neutrophils. *Biochem. J.* 237:111–116.
- Demaurex, N., G. P. Downey, T. K. Waddell, and S. Grinstein. 1996. Intracellular pH regulation during spreading of human neutrophils. *J. Cell Biol.* 133:1391–1402.
- Dunford, H. B. 1999. Heme Peroxidases. John Wiley & Sons, New York.
- Finocchiaro, L. M. E., E. S. Arzt, S. Fernandez-Castelo, M. Criscuolo, S. Finkelman, and V. E. Nahmod. 1988. Serotonin and melatonin synthesis in peripheral blood mononuclear cells: Stimulation by interferon- $\gamma$  as part of an immunomodulatory pathway. *J. Interferon Res.* 8:705–716.
- Finocchiaro, L. M. E., V. E. Nahmod, and J. M. Launay. 1991. Melatonin biosynthesis and metabolism in peripheral-blood mononuclear leukocytes. *Biochem. J.* 280:727–731.
- Fujimoto, S., N. Kawakami, and N. Ohara. 1993. Formation of hydroxyl radical by the myeloperoxidase NADH oxygen system. *Biol. Pharm. Bull.* 16:525–528.
- Furtmüller, P. G., C. Obinger, Y. Hsuanyu, and H. B. Dunford. 2000. Mechanism of reaction of myeloperoxidase with hydrogen peroxide and chloride ion. *Eur. J. Biochem.* 267:5858–5864.
- Ginis, I., and A. I. Tauber. 1990. Activation mechanisms of adherent human neutrophils. *Blood.* 76:1233–1239.
- Hampton, M. B., A. J. Kettle, and C. C. Winterbourn. 1998. Inside the neutrophil phagosome: oxidants, myeloperoxidase, and bacterial killing. *Blood.* 92:3007–3017.
- Hauser, M. J. B., and L. F. Olsen. 1998. The role of naturally occurring phenols in inducing oscillations in the peroxidase-oxidase reaction. *Biochemistry.* 37:2458–2469.
- Henderson, L. M., and J. B. Chappell. 1996. NADPH oxidase of neutrophils. *Biochim. Biophys. Acta.* 1273:87–107.
- Henzler, T., and E. Steudle. 2000. Transport and metabolic degradation of hydrogen peroxide in *Chara corallina*: model calculation and measurements with the pressure probe suggest transport of  $\text{H}_2\text{O}_2$  across water channels. *J. Exp. Bot.* 51:2053–2066.
- Jones, R. D., J. T. Hancock, and A. H. Morice. 2000. NADPH oxidase: a universal oxygen sensor? *Free Radic. Biol. Med.* 29:416–424.
- Kindzelskii, A. L., M. J. Zhou, R. P. Haugland, and H. R. Petty. 1998. Oscillatory pericellular proteolysis and oxidant deposition during neutrophil migration. *Biophys. J.* 74:90–97.
- Kindzelskii, A. L., and H. R. Petty. 2000. Extremely low frequency electric fields promote neutrophil extension, metabolic resonance and DNA damage during migration. *Biochim. Biophys. Acta.* 1495:90–111.
- Kirkor, E. S., and A. Scheeline. 2000. Nicotinamide adenine dinucleotide species in the horseradish peroxidase-oxidase oscillator. *Eur. J. Biochem.* 267:5014–5022.
- Klebanoff, S. J. 1991. Myeloperoxidase: occurrence and biological function. In *Peroxidases in Chemistry and Biology*. J. Everse, K. E. Everse and M. B. Grisham, editors. CRC Press, Boca Raton, FL. 1–35.
- Kummer, U., M. J. B. Hauser, K. Wegmann, L. F. Olsen, and G. Baier. 1997. Oscillations and complex dynamics in the peroxidase-oxidase reaction induced by naturally occurring aromatic substrates. *J. Am. Chem. Soc.* 119:2084–2087.
- Levy, R., O. Nagauker, E. Sikuler, T. L. Leto, and F. Schlaeffer. 1994. Elevated NADPH-oxidase activity in neutrophils from bile-duct-ligated rats; changes in the kinetic parameters and in the oxidase cytosolic factor p47. *Biochim. Biophys. Acta.* 1220:261–265.
- MacDonald, R. C., R. I. MacDonald, B. P. Menco, K. Takeshita, N. K. Subbarao, and L. R. Hu. 1991. Small-volume extrusion apparatus for preparation of large unilamellar vesicles. *Biochim. Biophys. Acta.* 1061:297–303.
- Matuszak, Z., K. Reszka, and C. F. Chignell. 1997. Reaction of melatonin and related indoles with hydroxyl radicals: EPR and spin trapping investigations. *Free Rad. Biol. Med.* 23:367–372.
- McCord, J. M. 2000. The evolution of free radicals and oxidative stress. *Am. J. Med.* 108:652–659.
- Mohan, R. F., and M. S. Jacobson. 1993. Inhibition of macrophage superoxide generation by dehydroepiandrosterone. *Am. J. Med. Sci.* 306:10–15.
- Morrey, K. M., J. A. McLachlan, C. D. Serkin, and O. Bakouche. 1994. Activation of human monocytes by the pineal hormone melatonin. *J. Immunol.* 153:2671–2680.
- Nakamura, S., K. Yokota, and I. Yamazaki. 1969. Sustained oscillations in a lactoperoxidase, NADPH and  $\text{O}_2$ -system. *Nature.* 222:794.
- Oehler, R., G. Weingartmann, N. Manhart, U. Salzer, M. Meissner, W. Schlegel, A. Spittler, M. Bergmann, D. Kandioler, S. Oismüller, H. M. Struse, and E. Roth. 2000. Polytrauma induces increased expression of pyruvate kinase in neutrophils. *Blood.* 95:1086–1092.
- Olsen, L. F., A. Lunding, F. R. Lauritsen, and M. Allegra. 2001. Melatonin activates the peroxidase-oxidase reaction and promotes oscillations. *Biochem. Biophys. Res. Commun.* 284:1071–1076.

- Petty, H. R., R. G. Worth, and A. L. Kindzelskii. 2000. Imaging sustained dissipative patterns in the metabolism of individual living cells. *Phys. Rev. Lett.* 84:2754–2757.
- Petty, H. R. 2001. Neutrophil oscillations: temporal and spatiotemporal aspects of cell behavior. *Immunol. Res.* 23:85–94.
- Recchioni, R., F. Marcheselli, F. Moroni, R. Gaspar, S. Damjanovich, and C. Pieri. 1998. Melatonin increases the intensity of respiratory burst and prevents L-selectin shedding in human neutrophils in vitro. *Biochem. Biophys. Res. Commun.* 252:20–24.
- Rom, W. N., and T. Harkin. 1991. Dehydroepiandrosterone inhibits the spontaneous release of superoxide radical by alveolar macrophages in vitro in asbestosis. *Environ. Res.* 55:145–156.
- Rosenspire, A. J., A. L. Kindzelskii, and H. R. Petty. 2000. Interferon- $\gamma$  and sinusoidal electric fields signal by modulating NAD(P)H oscillations in polarized neutrophils. *Biophys. J.* 79:3001–3008.
- Scheeline, A., D. L. Olson, E. P. Williksen, G. A. Horras, M. L. Klein, and R. Larter. 1997. The peroxidase-oxidase oscillator and its constituent chemistries. *Chem. Rev.* 97:739–756.
- Sevcik, P., and H. B. Dunford. 1991. Kinetics of the oxidation of NADH by methylene blue in a closed system. *J. Phys. Chem.* 95:2411–2415.
- Silva, S. O., V. F. Ximenes, L. H. Catalani, and A. Campa. 2000. Myeloperoxidase-catalyzed oxidation of melatonin by activated neutrophils. *Biochem. Biophys. Res. Commun.* 279:657–662.
- Sørensen, O., and N. Borregaard. 1999. Methods for quantitation of human neutrophil proteins: a survey. *J. Immunol. Methods.* 232:179–190.
- Tauber, A. I. 1987. Protein kinase C and the activation of the human neutrophil NADPH oxidase. *Blood.* 69:711–720.
- Tyagi, S. R., M. Tamura, D. N. Burnham, and J. D. Lambeth. 1988. Phorbol myristate acetate (PMA) augments chemoattractant-induced diglyceride generation in human neutrophils but inhibits phosphoinositide hydrolysis. Implications for the mechanism of PMA priming of the respiratory burst. *J. Biol. Chem.* 263:13191–13198.
- Whitcomb, J. M., and A. G. Schwartz. 1985. Dehydroepiandrosterone and 16  $\alpha$ -Br-epiandrosterone inhibit 12-O-tetradecanoylphorbol-13-acetate stimulation of superoxide radical production by human polymorphonuclear leukocytes. *Carcinogen.* 6:333–335.
- White, A., P. Handler, E. L. Smith, R. L. Hill, and I. R. Lehman. 1978. *Principles of Biochemistry*. McGraw-Hill, New York.
- Ximenes, V. F., L. H. Catalani, and A. Campa. 2001. Oxidation of melatonin and tryptophan by an HRP cycle involving compound III. *Biochem. Biophys. Res. Commun.* 298:130–134.
- Zhang, H., G. Squadrito, and W. A. Pryor. 1998. The reaction of melatonin with peroxynitrite: formation of melatonin radical cation and absence of stable nitrated products. *Biochem. Biophys. Res. Commun.* 251:83–87.